



Distribution and biomass of gelatinous zooplankton in relation to an oxygen minimum zone and a shallow seamount in the Eastern Tropical North Atlantic Ocean

Florian Lüskow^{a,b}, Bernd Christiansen^c, Xupeng Chi^{d,e}, Péricles Silva^f, Philipp Neitzel^d, Mollie E. Brooks^g, Cornelia Jaspers^{h,*}

^a Department of Earth, Ocean and Atmospheric Sciences, University of British Columbia, 2039–2207 Main Mall, Vancouver, British Columbia, V6T 1Z4, Canada

^b Institute for the Oceans and Fisheries, University of British Columbia, 2202 Main Mall, Vancouver, British Columbia, V6T 1Z4, Canada

^c Institute of Marine Ecosystem and Fishery Science, Universität Hamburg, Große Elbstraße 133, 22767, Hamburg, Germany

^d GEOMAR, Helmholtz Centre for Ocean Research Kiel, Düsterbrookweg 20, 24105, Kiel, Germany

^e Key Laboratory of Marine Ecology & Environmental Sciences, Institute of Oceanology, Chinese Academy of Sciences, Nanhai Road 7, Qingdao, 266071, China

^f Instituto Nacional de Desenvolvimento das Pescas, Cova da Inglesa, CP132, Mindelo, São Vicente, Cape Verde

^g National Institute of Aquatic Resources, Technical University of Denmark, Kemitorvet, 2800 Kgs. Lyngby, Denmark

^h Centre for Gelatinous Plankton Ecology & Evolution, National Institute of Aquatic Resources, Technical University of Denmark, Kemitorvet, 2800, Kgs. Lyngby, Denmark

ARTICLE INFO

Keywords:

Cape Verde Ocean Observatory
Ctenophore
Jellyfish
Oxygen minimum zone
Pyrosome
Senghor Seamount
Length-weight regressions
Deoxygenation
Global change

ABSTRACT

Physical and topographic characteristics can structure pelagic habitats and affect the plankton community composition. For example, oxygen minimum zones (OMZs) are expected to lead to a habitat compression for species with a high oxygen demand, while upwelling of nutrient-rich deep water at seamounts can locally increase productivity, especially in oligotrophic oceanic waters. Here we investigate the response of the gelatinous zooplankton (GZ) assemblage and biomass to differing oxygen conditions and to a seamount in the Eastern Tropical North Atlantic (ETNA) around the Cape Verde archipelago. A total of 16 GZ taxa (>1100 specimens) were found in the upper 1000 m with distinct species-specific differences, such as the absence of deep-living species *Atolla wyvillei* and *Periphylla periphylla* above the shallow seamount summit. Statistical analyses considering the most prominent groups, present at all stations, namely *Beroe* spp., hydromedusae (including *Zygocanna vagans*, *Halicreas minimum*, *Colobonema sericeum*, *Solmissus* spp.) and total GZ, showed a strong positive correlation of abundance with temperature for all groups, whereas oxygen had a weak negative correlation only with abundances of *Beroe* spp. and hydromedusae. To account for size differences between species, we established length-weight regressions and investigated total GZ biomass changes in relation to physical (OMZ) and topographic characteristics. The highest GZ biomass was observed at depths of lowest oxygen concentrations and deepest depth strata at the southeastern flank of the seamount and at two stations south of the Cape Verde archipelago. Our data suggest that, irrespective of their patchy distribution, GZ organisms are ubiquitous food web members of the ETNA, and their habitat includes waters of low oxygen content.

1. Introduction

Gelatinous zooplankton (GZ) belong to taxonomically and ecologically different groups of plankton organisms that are characterised by a fragile, transparent body texture, and mostly low carbon content (Kjørboe, 2013). They have been documented as important grazers (e.g. Décima et al., 2019), prey items (e.g. Diaz Briz et al., 2017; Ayala et al.,

2018), and facilitators of vertical carbon export (e.g. Lebrato and Jones, 2009). Despite an increasing interest in gelatinous organisms in the context of climate change, overfishing, and ecosystems alterations (as reviewed in Richardson et al., 2009), knowledge about their spatial distribution pattern including meso- and bathypelagic depths remains limited (e.g. Robison, 2004), especially in relation to oxygen minimum zones (OMZs) in the open ocean (but see Hauss et al., 2016; Hoving

* Corresponding author.

E-mail address: coja@aqu.dtu.dk (C. Jaspers).

<https://doi.org/10.1016/j.marenvres.2022.105566>

Received 16 April 2021; Received in revised form 15 January 2022; Accepted 19 January 2022

Available online 31 January 2022

0141-1136/© 2022 The Authors. Published by Elsevier Ltd. This is an open access article under the CC BY license (<http://creativecommons.org/licenses/by/4.0/>).

et al., 2020). This knowledge gap is primarily due to sampling difficulties using traditional nets and preservation problems of certain groups such as ctenophores (van Walraven et al., 2013), highlighting the importance of special handling procedures and live analyses of samples (for methodology see e.g. Haraldsson et al., 2013).

OMZs are defined as persistent water layers with significantly reduced oxygen concentration (see Diaz and Rosenberg, 2008), located, e.g., in boundary upwelling areas such as in the eastern tropical North and South Atlantic and Pacific Oceans (e.g. Karstensen et al., 2008). The OMZs in the north-eastern tropical Atlantic are not as oxygen depleted as compared to, for example, the Pacific, though their horizontal and vertical extent is expected to increase with global climate change (e.g. Karstensen et al., 2008). This is suggested to have large consequences for high oxygen-demanding species (e.g. Stramma et al., 2008), due to a habitat reduction. Naturally, OMZs occur in the open ocean at mesopelagic depths, particularly in areas of high surface productivity (e.g. Karstensen et al., 2008). In open oceans, OMZs are persistent, while productive coastal areas are characterised by seasonally occurring low oxygen conditions or hypoxia ($<2 \text{ mg O}_2 \text{ l}^{-1} \approx 62.5 \text{ } \mu\text{mol kg}^{-1}$) (see Diaz, 2001). For coastal areas, several GZ species have been documented to show high tolerance towards low dissolved oxygen (DO) concentrations (Kolesar et al., 2010; but see Lučić et al., 2019). Some scyphozoan jellyfish have even been shown to tolerate short-term anoxic events, where the DO concentration reaches zero (Thuesen et al., 2005). We hypothesise that GZ in open oceans are also tolerant towards OMZs, reflected in high abundances at low oxygenated water depths.

Apart from physical characteristics, topographic features can structure the composition, abundance and distribution of plankton communities. Seamounts, for example, interact with the surrounding flow regime (e.g., Lavelle and Mohn, 2010), which may lead to local upwelling and enhanced primary production in otherwise oligotrophic oceans (e.g. Leitner et al., 2021), or to the advection and retention of particles supporting biomass to different trophic levels (e.g. Morato et al., 2008; Hirsch et al., 2009). It can further be expected that deep-living GZ species, such as the scyphozoan jellyfish *Periphylla periphylla* will not be present above the shallow seamount topography. While *P. periphylla* is a large jellyfish, hydromedusae are often characterised by a small size. In order to account for the size differences between different GZ groups, we established length-weight regressions and compiled conversion factors to allow for estimating the carbon content of the most prominent groups and to calculate the total GZ biomass. Especially with regard to the carbon content, GZ groups show a large variability. While ctenophores have the lowest carbon content in relation to their wet weight (as reviewed in Kjørboe, 2013), scyphomedusae are characterised by a very high variability in carbon content, spanning a 2.5 orders of magnitude range in carbon weight relative to their wet weight (see meta-analyses in McConville et al., 2017). This illustrates that comparison of food web structure between regions needs to standardise abundance data into biomass (e.g. see Bar-On et al., 2018).

In this study, we quantitatively describe the gelatinous zooplankton assemblage from surface to mesopelagic depths in the Eastern Tropical North Atlantic in order to investigate if composition, abundances or biomass can be related to either physical variables (e.g. temperature, oxygen) or topographic characteristics (e.g. seamount summit, flanks or oceanic reference stations). Presented species- or group-specific length-weight and biomass conversions further allow for direct comparison of gelatinous zooplankton biomass across studies and allow for including gelatinous zooplankton into future food web models of this region.

2. Materials and methods

2.1. Study area

Sampling was carried out in the Eastern Tropical North Atlantic (ETNA) in the waters around the Cape Verde Islands between $18^{\circ}05.00'N$ – $12^{\circ}00.00'N$ and $24^{\circ}17.00'W$ – $20^{\circ}30.00'W$ in November and

December 2015 (Fig. 1) onboard *R/V Maria S. Merian* (cruise MSM49). This area has several seamounts, and one of them is the nearly conical-shaped shallow Senghor Seamount, which rises from 3300 m up to a small summit plateau c. 95 m below the surface (Denda and Christiansen, 2014). The water column in the surrounding area is characterised by an intermediate (40 – $100 \text{ } \mu\text{mol kg}^{-1}$) oxygen minimum zone (OMZ) that is roughly located between 100 and 500 m depth (Fig. 2). Its intensity varies, with the lowest oxygen concentrations (40 – $50 \text{ } \mu\text{mol kg}^{-1}$) observed southeast of Cape Verde (Brandt et al., 2015). Around the archipelago, several currents structure the pelagic realm: the North Equatorial Current to the north, the North Equatorial Counter Current to the south, and the Mauritanian Current to the east (Aristegui et al., 2009). Nine stations were selected to cover a wide area of the Cape Verdean waters, including i) the Senghor Seamount (grouped into Summit station (d) and Seamount Flank stations (Cc): NW flank, SE flank), ii) the open ocean OMZ in the southeast of the archipelago (stations (b): CVS1, CVS2, CVSE), hereafter referred to as Oceanic Reference South, and iii) open ocean reference stations with slightly higher dissolved oxygen (DO) concentrations at depth, north of the seamount, (stations (a): CVN, CVOO, Senghor Ref), hereafter referred to as Oceanic Reference North (Figs. 1 and 2).

2.2. Environmental parameters

At all stations, vertical profiles of temperature (T, °C), salinity (S), and DO concentration ($\mu\text{mol kg}^{-1}$) were taken using a CTD sea bird (SBE 19 plus) equipped with an oxygen sensor (SBE 43) and 24 Niskin sampling bottles. DO concentrations from the oxygen sensor were calibrated against measurements of water samples taken at 16 distinct depths using Winkler titration (Grasshoff, 1999). Data for the upper 1000 m are presented.

2.3. Specimen collection and processing

Gelatinous meso- and macrozooplankton (GZ; size between 0.2 mm and 20 cm; Sieburth et al., 1978) were sampled using i) a MOCNESS-1, equipped with a flowmeter (mesh size 335 μm ; 1 m^2 mouth opening; six depth layers: 0–50; 50–100; 100–200; 200–400; 400–600; 600–1000 m; with 88–2500 m^3 filtered per net), ii) a MOCNESS-10, equipped with a flowmeter (mesh size 1.5 mm; 10 m^2 mouth opening; four depth layers: 0–100; 100–400; 400–600; 600–1000 m; with 1494–21053 m^3 filtered per net) and iii) a WP3 net (non-filtering cod end, 1 mm mesh size, 1.1 m diameter, deployed at irregular intervals, non-quantitative for qualitative analyses only). Two MOCNESS-1 tows during day and two catches during night, along with one MOCNESS-10 tow during day and night, respectively, were conducted. Fewer samples were taken at Oceanic Reference North stations (CVOO, CVN) and the Seamount Summit station (Table 3). All nets were analysed for GZ organisms, while MOCNESS nets were quantitatively analysed, WP3 nets were only qualitative. The procedure for quantitative MOCNESS-1 and MOCNESS-10 analyses was as follows: first, all samples were scanned for large organisms (diameter $>15 \text{ cm}$), which were measured and removed before the entire sample was split into two halves by carefully shaking them 32 times in a modified Folsom plankton splitter (McEwen et al., 1954). Second, one-half of the split sample was immediately preserved in 4% borax-buffered formaldehyde-seawater solution for later laboratory analyses e.g. to establish GZ length-weight relationships and other general zooplankton analyses. Third, the other half of the split sample was directly analysed by identifying and sizing all GZ organisms on a light table within 60 min following collection to estimate abundance and sizes (see below). Gelatinous organisms were identified to the lowest possible taxonomic level using published identification keys (e.g. Mills and Haddock, 2007) and photographic identity confirmation by taxonomic experts. Sizes were assessed on a light table in a transparent tray using a calliper and measurements were rounded to the nearest mm. The four most frequently occurring hydromedusae (*Zygocanna vagans*,

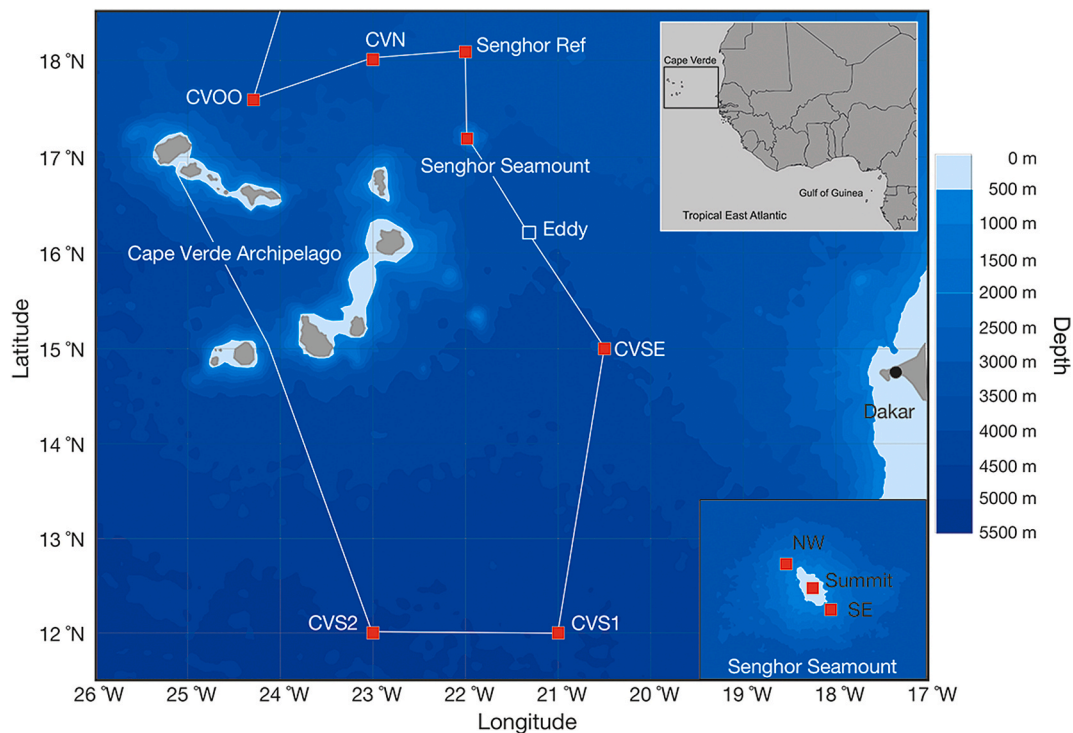


Fig. 1. Cruise track and sampling stations at the oxygen minimum zone, Senghor Seamount, and the oceanic reference stations in Cape Verdean waters (Eastern Tropical North Atlantic Ocean) in November and December 2015. Stations cluster as following – Oceanic Reference North (CVN, CVOO, Senghor Ref), Oceanic Reference South (CVS1, CVS2, CVSE), Seamount Flanks (Senghor NW, Senghor SE), and Seamount Summit (Senghor Summit).

Solmissus spp., *Colobonema sericeum*, *Halicreas minimum*) were pooled for the quantitative analyses, as they did not differ in their length-weight relationships (see Fig. 3 legend and results). *Pyrostremma agassizi* was the only quantified thaliacean present in large quantities. The sampling procedure was unsuited for appendicularians, which were not included in the analyses. Salps (i.e., *Salpa fusiformis* and *Thetys vagina*, based on picture identifications) occurred only sporadically due to their highly patchy distribution, and were therefore not included in the analyses. Also, siphonophores were not included in the analyses due to the difficulty to catch them intact. Count data from the live material analysed on board (50% of the original sample) were used for statistical analyses, accounting for water volume filtered and sub-sampling factor. Size measurements from live material analysed on board were used to estimate biomass of the GZ assemblage by applying our length-weight regressions, as outlined in the next section.

2.4. Length-weight measurement and biomass conversions

Gelatinous macrozooplankton (GZ) organisms preserved in 4% borax-buffered formaldehyd (half of the original sample, which was immediately preserved on board) were used to establish length-weight relationships (wet weight) for the most prominent groups (see Fig. 3). Within six months after the cruise, eight GZ taxa were analysed in the laboratory to establish length-weight relationships. First, samples were rinsed with fresh seawater (at the corresponding sample salinity) to remove surplus formalin before samples were transferred into sorting solution until analysis (Tranter, 1962). Upon analysis, animals were individually measured to the nearest mm with as little water as possible on a Petri dish using a calliper (total length in case of ctenophores and pyrosomes, diameter in case of medusae). Thereafter, animals were washed with distilled water for 1–2 min on a sieve before removing excess fluid with paper towels and wet weight (g) assessment using a precision balance (Sartorius LA620P). Length-weight relationships were established for the most prominent GZ groups encountered during the cruise, namely the scyphozoan jellyfish species *Atolla wyvillei*, the

hydromedusae *Zygocanna vagans*, *Solmissus* spp., *Colobonema sericeum*, *Halicreas minimum*, the ctenophores *Beroe* spp. and an undescribed cydippid, as well as the pyrosome *Pyrostremma agassizi* (see Fig. 3 and Tables 1 and 2). As length-weight regressions were assessed from formalin-preserved material, while animals were sized alive on board and used for quantitative analyses presented in this study, we conducted a literature review to confirm that the slopes of the individual length-weight regressions from preserved material did not significantly differ from unpreserved material (Fig. 3D, Table 1). For all investigated groups, we did not find a significant difference of individual slopes (using a separate slopes model) comparing live with preserved material, suggesting that preservation is a volumetric problem. Slope differences between species or taxonomic groups are thus likely due to differences related to their structure such as appendices (e.g. tentacles) and shapes (e.g. barrel versus ball). Therefore, we could directly assess wet weight from unpreserved sizes without approximation of shrinkage effects. Sizes (mm) of all measured individuals on board were used to calculate wet weights (g). We used literature conversion factors to estimate carbon content from wet weight directly (Table 2) following Kiørboe (2013) and McConville et al. (2017). Note: Length-weight regression for hydromedusae is presented as grouped hydromedusae due to the limited sample size within the class Hydrozoa (*Colobonema sericeum* (n = 4), *Halicreas minimum* (n = 7), *Solmissus* spp. (n = 8), *Zygocanna vagans* (n = 4)) and the confirmation that the individual slopes of the generated length-weight regressions did not significantly differ ($P > 0.3$) (pooled overall regression for hydromedusae see Table 1 and Fig. 3).

In rare cases where sizes were not assessed, average sizes of the same species at the respective station were used as proxy for carbon content estimations. For very rarely encountered species, where no length-weight relationship was established, we used regressions of closely related species. In detail, we used the here generated regressions for *A. wyvillei* for other scyphomedusae (i.e. *Periphylla periphylla*), the pooled hydromedusae regression for six unidentified hydromedusae (see below), *Liriope tetraphylla* and *Aegina* spp. as well as the regression for the ctenophore *Beroe* spp. for *Hormiphora* spp. and four unidentified

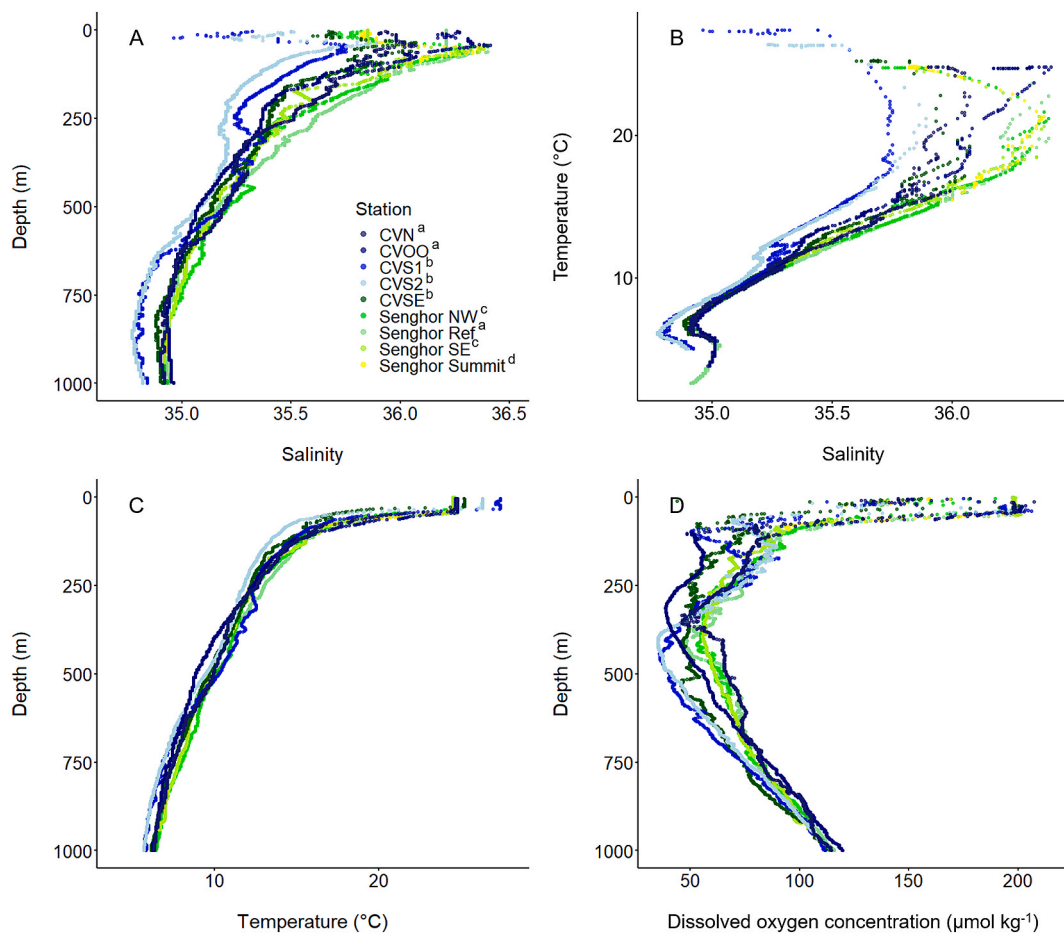


Fig. 2. Hydrography with depth profiles of A: salinity, B: temperature-salinity, C: temperature (T , $^{\circ}\text{C}$), and D: dissolved oxygen concentration (DO , $\mu\text{mol kg}^{-1}$) in the upper 1000 m. Stations cluster as following a: Oceanic Reference North (CVN, CVOO, Senghor Ref), b: Oceanic Reference South (CVS1, CVS2, CVSE), c: Seamount Flanks (Senghor NW, Senghor SE), and d: Seamount Summit (Senghor Summit).

ctenophores (see below). Two individuals of the ctenophore species *Ocyropsis crystallina*, which were encountered at station CVOO between 100 and 200 m, were not included in biomass estimates due to lack of size estimates. In total, four ctenophores (at station CVOO 0–50 m, 200–400 m, 600–1000 m and CVS2 600–1000 m) and six hydromedusae (at station SNW 0–100 m, SE 50–100 m and 600–1000 m as well as three at Seng Ref station at 200–400 m depth) have not been identified to higher taxonomic level and are only included in total GZ biomass estimates. Siphonophores were not included in total GZ biomass estimates due to their fragility and difficulty to catch intact colonies, but were present in 46 nets. Only one intact stem of *Physophora hydrostatica* was sampled at station CVS1 (200–400 m).

2.5. Statistical analyses of abundance

To quantify how abundances varied with environment and gear, we separately modelled counts of the two most abundant species groups in the data set (i.e. *Beroe* spp. and grouped hydromedusae) and the total count of all GZ species using generalised linear mixed models (GLMMs) with the *glmmTMB* package in the R environment (Brooks et al., 2017; R Core Team 2020). All models included a random effect of tow to account for possible correlations among the multiple observations within each tow as well as a random effect of station to account for possible differences among spatial locations that were not captured by the environmental covariates. All models contained an offset of the log of the volume of water filtered (m^3) to control for differences in the filtered water volume for the two gear types. This use of an offset in the models produces estimates that can be interpreted in terms of counts per unit

volume. It is common in GLMs and GLMMs of count data to use the log of sampling effort, sampling area, or sampling volume as an offset in a model with a log-link because this has the desired mathematical result of controlling for that nuisance variable, while allowing the count data to be modelled as integers as they were observed (Hardin and Hilbe, 2007; Bolker, 2015). We quantified the impact of median DO concentration ($\mu\text{mol O}_2 \text{ kg}^{-1}$), median temperature ($^{\circ}\text{C}$), and median salinity per depth stratum, depth (m), time of the day (day versus night), and gear type (MOCNESS-1 versus MOCNESS-10). Continuous variables were scaled to have mean zero and unit variance in the whole data set so that estimated coefficients from GLMMs could be compared within a model as well as between different models (Schielzeth, 2010). Before plotting, estimated regression coefficients from the GLMMs were converted to ratios for easier interpretation. For example, the estimated regression model coefficient of Oxygen on *Beroe* spp. abundance was -0.52 and this can be converted to $\exp(-0.52)$, which leads to a value of 0.59, meaning that increasing oxygen by 1 standard deviation from the mean (while all other continuous variables are at their means) will produce 59% of the count expected when all continuous variables are at their means (see electronic supplement for more detail). In preliminary analyses, we found that models with a *nbinom2* distribution frequently had convergence problems both for the whole data set and for individual species groups, so we used the *nbinom1* distribution. The *nbinom1* distribution assumes that variance increases linearly with the mean, whereas *nbinom2* assumes that variance increases quadratically with the mean (Hardin and Hilbe, 2007). Both distributions allow for overdispersion. We also checked that the distribution adequately handled zeros in the count data using the *DHARMA* package (Hartig, 2020). Using this

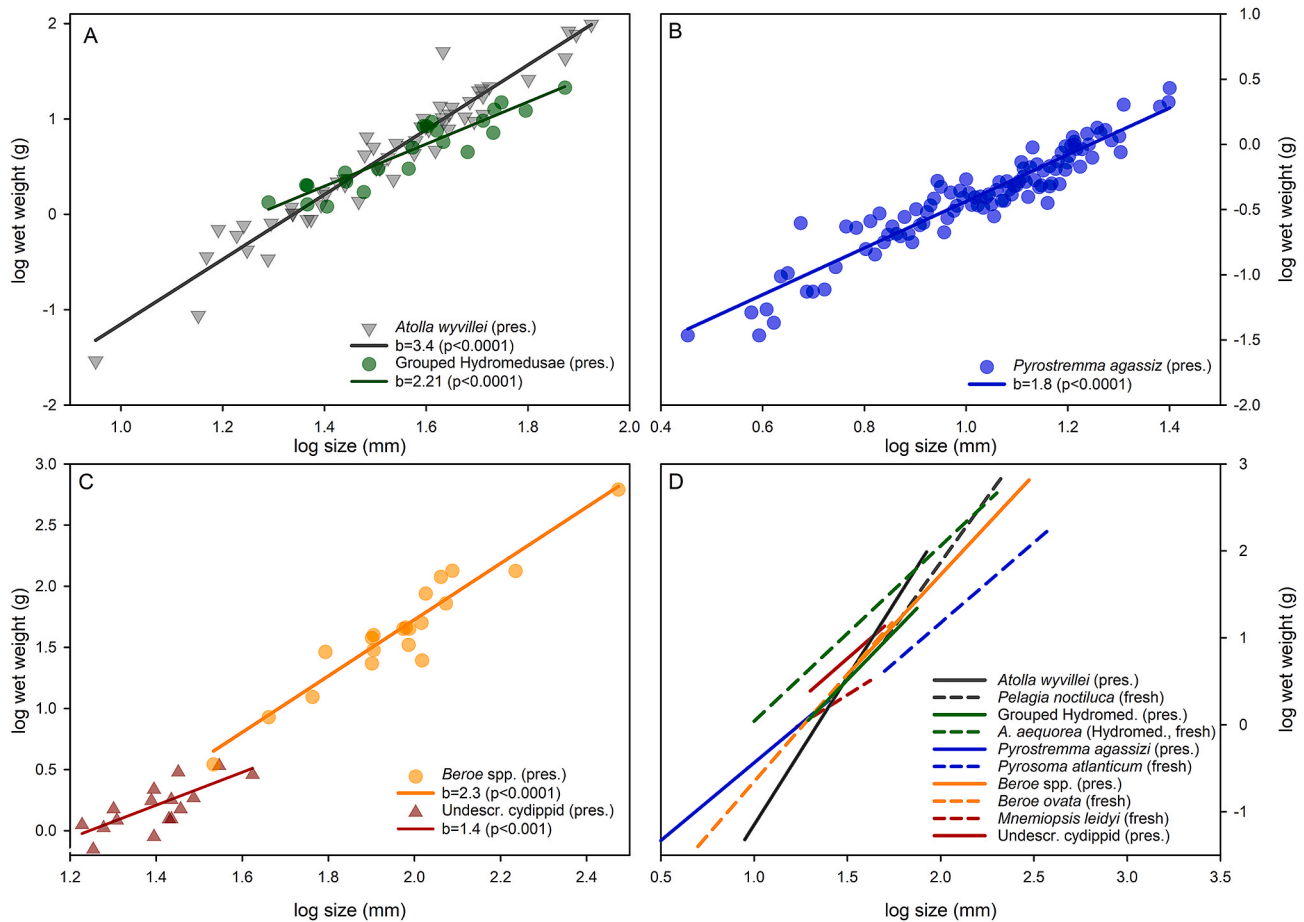


Fig. 3. Length-weight regressions of different gelatinous zooplankton groups (A–C) with slope comparison of preserved versus live material (D). Length-weight regressions of formalin-preserved A) scypho- (grey) and hydromedusae (green), B) pyrosomes (blue) and C) ctenophores (orange, Beroidea; red, Cydippida). Slope comparison of preserved (solid) versus fresh (hatched) material confirmed that slopes did not significantly differ within taxonomic groups (scyphomedusae, $P = 0.1$; hydromedusae, $P = 0.2$; pyrosomes, $P = 0.8$; Beroidea, $P = 0.7$, Ctenophora, $P = 0.1$). For details see Table 2. (For interpretation of the references to colour in this figure legend, the reader is referred to the Web version of this article.)

Table 1

Power regression parameters for length-weight relationships $WW(g) = Y_0 \times size (mm)^b$ of 4% borax-buffered formaldehyde-preserved gelatinous zooplankton organisms from the Eastern Tropical North Atlantic Ocean (see Fig. 3).

	Slope (b)	SE	Intercept (Y_0)	Size range (mm)	R^2	F	P
Hydromedusae, grouped	2.21	± 0.19	0.002	20–75	0.86	131	<0.0001
<i>Atolla wyvillei</i>	3.40	± 0.12	0.00003	9–84	0.94	822	<0.0001
<i>Beroe</i> spp.	2.30	± 0.17	0.001	35–300	0.91	179	<0.0001
Unid. cydippid ctenophore	1.35	± 0.32	0.021	17–42	0.56	18	0.001
<i>Pyrostremma agassizi</i>	1.79	± 0.06	0.006	3–25	0.90	912	<0.0001

Table 2

Conversion factors used to estimate carbon content (C) based on wet weight (WW) measurements for relevant groups encountered in the Eastern Tropical North Atlantic Ocean with number of conversion factors (n), average C % of WW and standard deviation (SD) (compiled from McConville et al., 2017).

Taxon	Class/Species	n	C % WW	SD
Thaliacea	<i>Pyrosoma atlanticum</i>	1	1.43	
Hydrozoa		13	0.42	± 0.28
	Narcomedusae	3	0.27	± 0.19
	Leptothecatae	5	0.43	± 0.38
	Trachymedusae	5	0.51	± 0.23
Scyphozoa	<i>Atolla wyvillei</i>	1	0.77	
Ctenophora	<i>Beroe</i> spp.	3	0.20	± 0.04
	Cydippida	5	0.42	± 0.32

package, the adequacy of the distribution in the fitted model is checked by simulating data sets from the fitted model and comparing the number of zeros and dispersion to those from the observed data (Hartig, 2020).

For each species group, we first fit a full model with all terms. Then, we used Akaike Information Criterion corrected for small sample size (AICc) to compare all sub-models (i.e. all possible subsets of the fixed effects), where each sub-model contained the offset and random effects described above (Whittingham et al., 2006). We did this using the *MuMIn* package in R because it allows the comparison of all sub-models to be done in an automated way (Barón, 2019). The set of sub-models contained models with terms dropped from the full model, which effectively represent null hypotheses wherein the dropped covariate has no relationship with abundance. We considered models with $\Delta AICc < 7$ to represent ecological plausible hypotheses (Burnham et al., 2011). We examined estimated effects with confidence intervals in the full

Table 3

Average gelatinous macrozooplankton abundance (ind. 1000 m⁻³) of the upper 1000 m of the water column, caught in the Eastern Tropical North Atlantic around Cape Verde archipelago during Nov/Dec 2015. Region, station name, number of MOCNESS-1/10 net tows (#) and bottom depths are indicated. Anthozoan larvae were only caught at Oceanic Reference station CVS2, while the ctenophore *Velamen parallelum* has only been caught once with the WP3 net at Oceanic Reference South (CVSE) station. Note: *Zygocanna vagans*, *Halicreas minimum*, *Colobonema sericeum*, *Solmissus* spp., are grouped as one size-weight relationship has been employed (see Table 1).

	Station region	Oceanic Reference North			Summit	Seamount Flanks		Oceanic Reference South		
	Station name	CVOO	CVN	Senghor Ref	Senghor S.	Senghor NW	Senghor SE	CVSE	CVS1	CVS2
	MOCNESS-1/-10 tow (#)	4/1	1/1	4/2	4/0	4/2	4/2	4/2	4/2	4/2
	Bottom depth (m)	3500	3400	3300	100	1000	1000	4200	4700	4900
Higher taxon	Species	Abundance (ind. 1000 m ⁻³)								
CTENOPHORA										
Nuda	<i>Beroe</i> spp.	0.72 ± 2.64	3.18 ± 4.65	2.29 ± 4.80	4.81 ± 8.16	1.50 ± 2.85	1.65 ± 3.81	0.85 ± 2.28	0.80 ± 1.78	0.70 ± 1.96
	<i>Hormiphora</i> spp.	0.13 ± 0.71	0.00 ± 0.00	0.00 ± 0.00	2.90 ± 7.10	0.11 ± 0.63	0.03 ± 0.18	0.00 ± 0.00	0.35 ± 2.00	0.00 ± 0.00
Tentaculata	<i>Ocyropsis crystallina</i>	0.04 ± 0.22	0.00 ± 0.00	0.00 ± 0.00	0.00 ± 0.00	0.00 ± 0.00	0.00 ± 0.00	0.00 ± 0.00	0.00 ± 0.00	0.00 ± 0.00
	Undescribed cydippid	0.26 ± 0.81	0.00 ± 0.00	0.06 ± 0.25	0.00 ± 0.00	0.02 ± 0.09	0.03 ± 0.10	0.52 ± 1.24	1.68 ± 3.23	0.19 ± 0.73
CNIDARIA										
Scyphozoa	<i>Atolla wyvillei</i>	0.01 ± 0.05	0.46 ± 1.12	0.39 ± 1.01	0.00 ± 0.00	0.10 ± 0.27	0.10 ± 0.29	0.16 ± 0.42	0.17 ± 0.44	0.12 ± 0.49
	<i>Periphylla periphylla</i>	0.00 ± 0.02	0.30 ± 0.74	0.02 ± 0.12	0.00 ± 0.00	0.02 ± 0.09	0.00 ± 0.00	0.00 ± 0.00	0.01 ± 0.05	0.00 ± 0.00
Hydrozoa	<i>Aegina</i> spp.	0.00 ± 0.00	0.00 ± 0.00	0.00 ± 0.00	0.00 ± 0.00	0.00 ± 0.00	0.00 ± 0.00	0.09 ± 0.47	0.00 ± 0.00	0.00 ± 0.00
	<i>Liriope tetraphylla</i>	0.00 ± 0.00	0.00 ± 0.00	0.00 ± 0.00	0.00 ± 0.00	0.00 ± 0.00	0.13 ± 0.75	0.01 ± 0.03	0.47 ± 2.64	0.32 ± 1.80
	<i>Physophora hydrostatica</i>	0.00 ± 0.00	0.00 ± 0.00	0.00 ± 0.00	0.00 ± 0.00	0.00 ± 0.00	0.00 ± 0.00	0.00 ± 0.00	0.08 ± 0.46	0.00 ± 0.00
	Grouped Hydromedusae	2.41 ± 9.97	0.96 ± 2.35	0.68 ± 1.71	1.52 ± 3.73	0.15 ± 0.53	1.83 ± 5.28	2.43 ± 4.90	3.38 ± 8.37	2.05 ± 4.21
TUNICATA										
Thaliacea	<i>Pyrostremma agassizi</i>	1.48 ± 4.59	0.48 ± 1.18	0.34 ± 1.87	4.63 ± 7.51	0.34 ± 1.58	14.33 ± 78.1	0.08 ± 0.26	60.30 ± 141.0	4.39 ± 9.21

model because it was within 7 AICc units of the most parsimonious model (Tables S1–S3) and it gives accurate 95% confidence intervals (Dormann et al., 2018).

3. Results

3.1. Oceanographic conditions

Based on overall station characteristics (oxygen minima, topographic features, location) the nine sampling stations could be grouped into Oceanic Reference North (CVN, CVOO, Senghor Ref, with minimum dissolved oxygen (DO) concentrations $\geq 50 \mu\text{mol kg}^{-1}$), Seamount Summit (Senghor Seamount, DO concentrations $> 100 \mu\text{mol kg}^{-1}$), Seamount Flanks (Senghor NW, Senghor SE, DO concentrations $> 50 \mu\text{mol kg}^{-1}$), and Oceanic Reference South (CVS1, CVS2, CVSE, with DO concentrations $> 45 \mu\text{mol kg}^{-1}$) stations (Figs. 1 and 2). However, this grouping was only used for gross comparison of biomasses between the regions and not introduced into the statistical analyses (see section 3.4). In general, the surface layer extended to about 50 m (Fig. 2), characterised by a weak pycnocline. Surface temperatures ranged between 24.5 and 27.4 °C and rapidly decreased below 150 m with the minimum temperature observed at the deepest sampling depth of 1000 m (range: 6.4–6.6 °C, Fig. 2). Overall, low DO concentrations were reached at depths between 270 and 550 m. Oceanic Reference South stations showed the lowest DO concentrations throughout the study area of $\geq 45 \mu\text{mol kg}^{-1}$, also characterised by a shallower upper limit of the DO minimum zone. In detail, for those stations DO minimum depth layers extended over several hundred meters from 100 to 510 m for station CVS1, from 70 to 420 m for station CVS2, and from 75 to 530 m for station CVSE (Fig. 2).

3.2. Gelatinous zooplankton distribution pattern

We sampled > 1100 specimens from at least 16 taxa using quantitative MOCNESS tows in the upper 1000 m of the water column, though most of those taxa were only infrequently encountered (Table 3). The shallowest seamount station (i.e. summit) was characterised by a faunal assemblage, which qualitatively differed from the set of species found at the seamount flank and oceanic reference stations, especially by lacking deep-living species such as the scyphomedusae *Atolla wyvillei* or *Periphylla periphylla*. In contrast, the hydromedusae *Zygocanna vagans*, *Halicreas minimum*, *Colobonema sericeum*, *Solmissus* spp., the ctenophore *Beroe* spp. as well as an undescribed cydippid ctenophore occurred region-wide (Table 3). Even though the tunicate *Pyrostremma agassizi* was found at all nine stations, its abundance was one to two orders of magnitude higher at the SE compared to the NW flank stations of the seamount, irrespective of similar sampling effort. Abundances of *P. agassizi* peaked at Oceanic Reference South station CVS1 (Table 3).

In addition to the qualitative description of the gelatinous zooplankton (GZ) assemblage, we investigated specific distribution patterns of key GZ groups in relation to physical and topographic characteristics. To do so, we focussed our statistical analyses on the most prominent groups, namely *Beroe* spp., grouped hydromedusae: *Zygocanna vagans*, *Halicreas minimum*, *Colobonema sericeum*, *Solmissus* spp. as well as total GZ abundance. Statistical analyses were performed using GLMMs, with AICc-based model selection. Our analyses confirmed that in all cases (*Beroe* spp., grouped hydromedusae: *Zygocanna vagans*, *Halicreas minimum*, *Colobonema sericeum*, *Solmissus* spp. and total GZ abundance), the full model containing all covariates of interest had < 7 delta AICc. Hence, our full model was selected, with all variables being of plausible ecological importance, for explaining observed abundance patterns (Tables S1–S3). Plots of estimated effects of oxygen,

temperature, salinity, depth, time of the day and gear along with 95% confidence intervals are shown in Fig. 4. Continuous variables were scaled to have mean zero and unit variance in the whole data set, so that estimates could directly be compared within a model as well as between different models (Fig. 4), following Schielzeth (2010). The models show a strong effect of gear for all three investigated groups, with regression model coefficient estimates ranging between -0.9 and -1.7 (Tables S1–S3), meaning that, per unit volume, MOCNESS-10 gear retains 19–40% of the number of specimens that MOCNESS-1 gear

retained (Fig. 4). For all investigated groups, higher volume-specific abundances were found in the MOCNESS-1 net. Hence, the larger MOCNESS-10, which filtered one order of magnitude larger water volumes, led to significantly lower GZ counts retained per volume filtered (Fig. 4). Additionally, temperature showed a strong positive correlation with all three groups, as coefficient estimates ranged between 0.9 and 1.6 (see Tables S1–3), while oxygen had a weak negative correlation with *Beroe* spp. and grouped hydromedusae abundances (Fig. 4). We observed a positive relationship between depth and *Beroe* spp. abundances (Fig. 4).

3.3. Length-weight relationships

We established length-weight relationships for several gelatinous zooplankton (GZ) groups, belonging to hydromedusae, scyphomedusae, pyrosomes and two ctenophore groups (Table 2, Fig. 3). As relationships were established from 4% borax-buffered formaldehyde-preserved material, while animals were sized alive on board, we conducted a literature review and compared the slopes of length-weight regressions from live and preserved material (see Fig. 3). We found that no significant difference could be detected comparing slopes of preserved versus live material for the individual groups. Therefore, scaling of size and wet weight remains constant and can be expressed by a common slope, irrespectively of preservation status. In detail, our analyses showed that the slope did not differ significantly between preserved and live tissue of i) grouped hydromedusae with the hydromedusa *Aequorea aequorea* (Buecher et al., 2001) ($P = 0.23$), ii) scyphozoans *A. wyvillei* with *Pelagia noctiluca* (Lilley et al., 2014) ($P = 0.1$), iii) the pyrosome *Pyrostremma agassizi* with *Pyrosoma atlanticum* (Henschke et al., 2019) ($P = 0.83$), iv) the ctenophore *Beroe* spp. with *Beroe ovata* (Svetlichny et al., 2004) ($P = 0.65$) and v) the undescribed cydippid with *Mnemiopsis leidyi* (Kremer and Nixon, 1976) ($P = 0.1$). Pyrosome regression provided in Henschke et al. (2019) of $WW(g) = 0.0013 TL(mm)^2 + 0.0151 TL(mm)$ was used to simulate data, which were then re-analysed, as size and weight is expected to follow a power relationship instead. The resulting regression between wet weight (WW, g) and total length (mm) is: $WW(g) = 0.003 \times TL(mm)^{1.83}$ ($P < 0.0001$) and corresponds well with re-analyses of extracted data from their publication in the size range of 40–375 mm, leading to the power regression coefficients: intercept (Y_0) = 0.003, slope (b) = 1.84 ± 0.06 ($R^2 = 0.86$, $P < 0.0001$).

Slopes and intercepts of Trachymedusae, Leptothecata, and Narcomedusae regressions did not differ significantly from each other ($P > 0.3$) and could therefore be expressed by one overall hydromedusae regression (power function $b = \text{slope}$, $Y_0 = \text{intercept}$) with $b = 2.3$, $Y_0 = -6.7$, $R^2 = 0.90$, $P < 0.0001$.

3.4. Biomass distribution of gelatinous zooplankton

Highest gelatinous zooplankton (GZ) biomass of $141 \text{ mg C } 1000 \text{ m}^{-3}$ was encountered at Oceanic Reference South stations (28.2 mg C m^{-2}) in the low oxygen layer at 400–600 m depth and in surface waters of the upper 100 m at Oceanic Reference North and South stations with an average biomass of 14.8 mg C m^{-2} and 13.8 mg C m^{-2} , respectively. Also, the depth layer of 600–1000 m at south eastern seamount flank stations showed high average integrated total GZ biomass of 39 mg C m^{-2} or $97.6 \text{ mg C } 1000 \text{ m}^{-3}$ (Fig. 5). For details, all biomass calculations and values can be found in the Supplementary raw data sheet.

3.5. Rare gelatinous zooplankton species encounters

Several other GZ species have been collected infrequently either by oblique MOCNESS-1 and MOCNESS-10 tows or qualitative vertical WP3 tows. Vertical WP3 tows usually sampled the upper 200 m with a lower towing speed (0.2 m s^{-1} versus $1 \text{ m s}^{-1} \approx 2 \text{ kn}$), but only the fragile cestid ctenophore *Velamen parallelum* (see Table 3 legend) was caught by the WP3 net alone ($n = 1$). Also, the narcomedusae *Aegina* spp. was collected

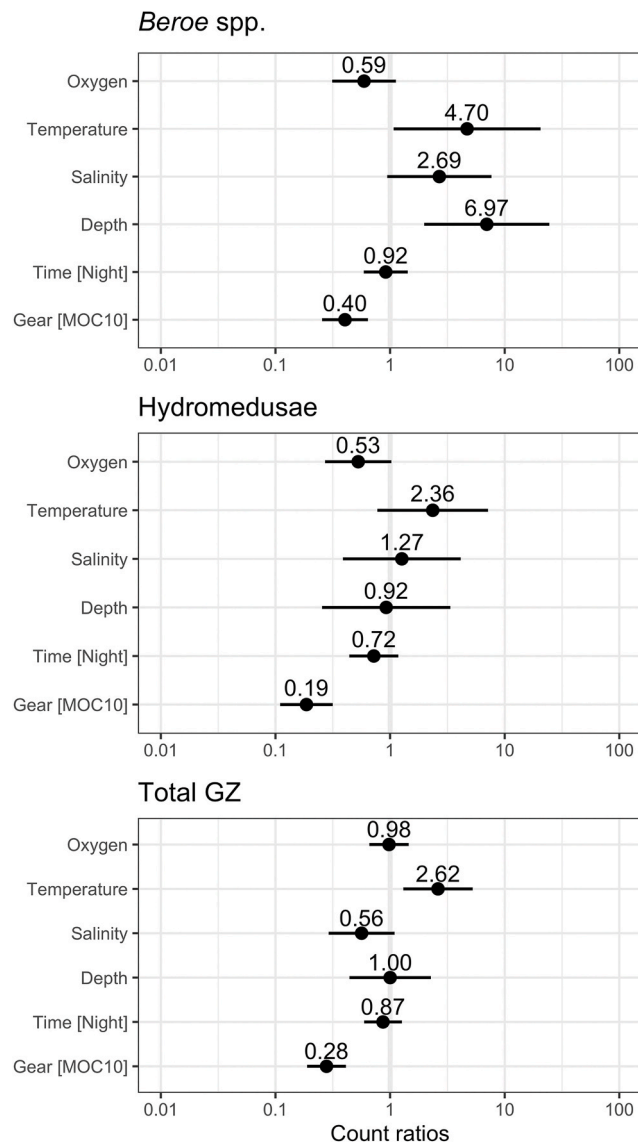


Fig. 4. Estimates and 95% Wald confidence intervals for the effects of covariates on abundance of *Beroe* spp. (upper panel), grouped hydromedusae (middle panel), and total gelatinous zooplankton (GZ, lower panel). Estimated regression coefficients from negative binomial GLMMs were converted to ratios for easier interpretation. A count ratio below 1 indicates that abundance is reduced by that covariate, whereas a count ratio above 1 leads to a higher abundance. For example, increasing temperature by one standard deviation would lead to 4.7 times the *Beroe* spp. count than at the mean temperature, while increasing oxygen by one standard deviation would lead to 0.59 times the *Beroe* spp. count than at the mean oxygen. Also, *Beroe* spp. counts in MOCNESS-10 gear are 40% of what they would be from MOCNESS-1 gear. Fixed effects were median dissolved oxygen conditions (Oxygen), median temperature (Temperature), median salinity (Salinity), mean depth (Depth), night versus day sampling (Time), and gear with MOCNESS-1 versus MOCNESS-10 (Gear). Visualised following Lüdecke (2021).

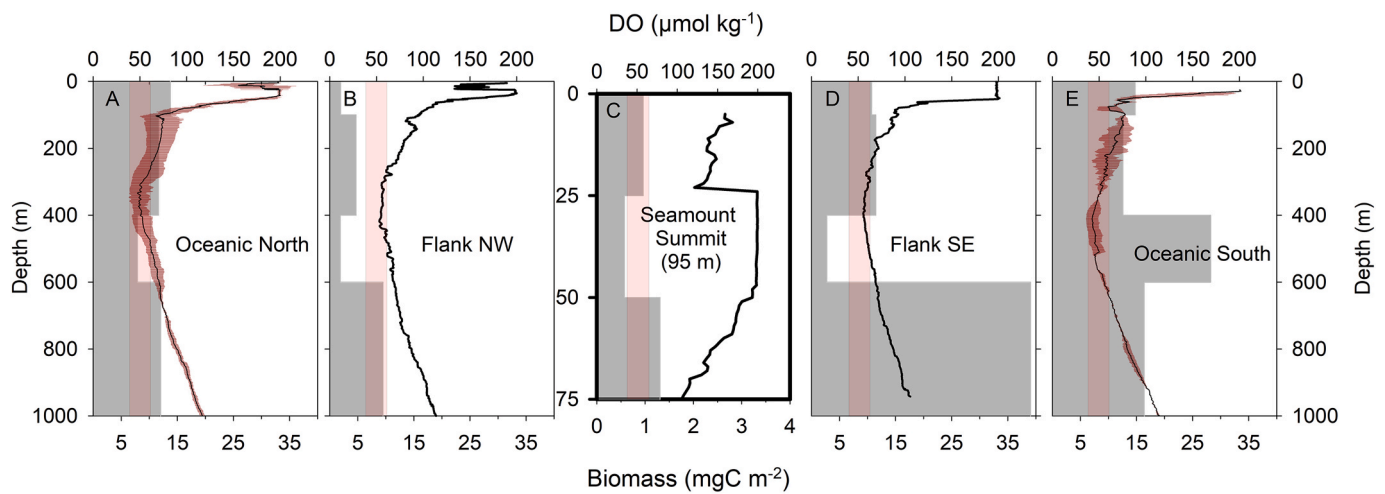


Fig. 5. Average total gelatinous zooplankton biomass (mg C m^{-2}) per depth layer (grey bar), without considering siphonophores. Stations have been grouped into regions as Oceanic Reference North, Seamount Flanks (north-west, NW and south-east, SE), Seamount Summit (bottom depth of c. 95 m), and Oceanic Reference South stations. Dissolved oxygen (DO) profiles are indicated as average (black line) \pm SD (dark red) and oxygen minimum layer of 40–60 $\mu\text{mol O}_2 \text{ kg}^{-1}$ indicated by transparent red box. Note: Scale for Seamount Summit station differs (C). (For interpretation of the references to colour in this figure legend, the reader is referred to the Web version of this article.)

only once in the Oceanic Reference South cluster by the MOCNESS-1. Salps were sporadically encountered, especially at the Oceanic Reference South stations. The tentaculate ctenophore *Hormiphora* spp. was collected with vertical and towed net types in low numbers throughout the study area (Table 2). Another ctenophore, *Ocyropsis crystallina*, was only observed at the Oceanic Reference North, while the limnomedusa *Liriope tetraphylla* was collected both at the seamount and the Oceanic Reference South stations. A single intact specimen of the siphonophore *Physophora hydrostatica* as well as anthozoan larvae were encountered at the Oceanic Reference South stations. As siphonophores are seldom caught complete, they were not included in the analyses, but present in all regions (41 observations).

4. Discussion

4.1. Oxygen and temperature relations with key GZ groups

Low oxygen concentrations can set limits to the distribution of high oxygen demanding species such as fish (Stramma et al., 2008), while it has been shown that most gelatinous zooplankton (GZ) organisms can tolerate low oxygenated waters (Purcell et al., 2001; Breitburg et al., 2003) and even survive short-term anoxia (Thuesen et al., 2005). Investigating the GZ assemblages in the Eastern Tropical North Atlantic (ETNA) during November–December 2015, we found that total GZ abundance is not significantly correlated with oxygen concentration. However, the pooled group of hydromedusae (i.e. *Zygocanna vagans*, *Halicreas minimum*, *Colobonema sericeum*, and *Solmissus* spp.) and the ctenophore *Beroe* spp. showed a weak negative correlation between oxygen concentration and abundances. This led to observed higher densities of these groups at depths characterised by low dissolved oxygen concentrations. Similar results were obtained by a towed video system during the investigation, where some hydromedusae species, but not *Beroe* spp., were found to be more common in oxygen minimum zones (OMZs; Hoving et al., 2020). In agreement with our results, it has been shown that 37% of the observed hydromedusae in Monterey Bay occurred in oxygen minimum layers. This included species such as *H. minimum* and *Solmissus* spp. (as reviewed in Purcell et al., 2001), which were found to show higher abundances under low oxygen conditions also in our study. In contrast to our observations, Hoving et al. (2020) found that *Beroe* spp. was distributed in the lower oxycline, but not the OMZ. This difference could be due to methodological differences in pooling of sampling depths, which might have masked some effects.

The oxygen conditions observed in our investigation ($\geq 45 \mu\text{mol kg}^{-1}$) are one order of magnitude higher compared to OMZs associated to highly productive anticyclonic modewater eddies (ACME) in the same area ($\geq 3.75 \mu\text{mol kg}^{-1}$, see Hauss et al., 2016). Within those eddies, GZ have been found to reside within the OMZ core without showing signs of diel vertical migration to higher oxygenated waters. Similarly, a global GZ biomass analysis indicates that relatively high biomass is maintained at low DO concentrations and hypoxic conditions, while overall GZ biomass increases with rising DO concentrations (Lucas et al., 2014). This suggests that GZ might be less severely affected by global deoxygenation due to climate change, as indicated for coastal waters, where copepod and anchovy populations were reduced during deoxygenation events, while GZ thrived (Slater et al., 2020).

In contrast to oxygen, we found a strong positive correlation of abundance with temperature for all investigated groups, namely *Beroe* spp. and the pooled hydromedusae (*Zygocanna vagans*, *Halicreas minimum*, *Colobonema sericeum*, *Solmissus* spp.) as well as total GZ. This indicates that higher GZ abundances are reached at higher temperatures. Similarly, Lucas et al. (2014) found a positive correlation between cnidarian biomass and temperature in the North Atlantic. Accordingly, GZ are expected to be favoured under global warming (Richardson et al., 2009), but the mechanistic understanding of the effects of temperatures on GZ in open ocean ecosystems needs to be studied in dedicated experiments. One mechanism might be faster growth and higher reproduction rates under warmer conditions, as shown for larvaceans (pelagic tunicates), which reach a minimum generation time of 1 day in tropical waters (Hopcroft and Roff, 1995).

4.2. Influence of sampling gear and volume filtered

Sampling gear type had a strong influence on all investigated gelatinous zooplankton (GZ) group abundances, with the strongest statistical effect size for the hydromedusae *Zygocanna vagans*, *Halicreas minimum*, *Colobonema sericeum*, *Solmissus* spp. Because the models accounted for the effect of sampling gear, this should have no impact on our statistical results for other covariates such as oxygen and temperature, unless there was an unobserved interaction between gear retention rate and an environmental covariate. We found that the finer meshed net (335 μm versus 1500 μm), after controlling for filtering one order of magnitude less water, leads to higher volume-specific abundances. Intuitively, one would expect that filtration of larger water volumes would lead to the inclusion of rare taxa and more reliable count data.

However, for gelatinous taxa, a trade-off between mesh size and filtered water seem to exist in general. The filtration of large volumes along with coarser meshed nets leads to damage of specimen during catch and even loss through the mesh. This has been described for GZ by comparing macrozooplankton trawls with Multinet tows, where the latter led to abundances, two orders of magnitude higher compared to large, coarse meshed trawls (Hosia et al., 2017). In our study, gear had a larger effect on hydromedusae compared to *Beroe* spp. and total GZ, which may be caused by their fragile structure (Remsen et al., 2004; Skjoldal et al., 2013). Delicate ctenophores of the order Cestida were extremely rare during the investigation and only caught once by a dedicated GZ vertical WP3 net tow at the Oceanic Reference South station CVSE. As highlighted by Hosia et al. (2017), different net types and water volumes should be combined for including rare and rigid GZ members such as scyphozoans as well as fragile ctenophores. Finer meshed nets are important to account for the small-sized hydromedusae.

4.3. Gelatinous zooplankton distribution pattern in relation to topographic features and daytime

The seamount summit was characterised by a minimum water depth of only c. 95 m, compared to the seamount flank stations above bottom depths of 1000 m. In accordance, the deep-living jellyfish species *P. periphylla* and *A. wyvillei* only occurred sporadically at the seamount flanks (between 400 and 1000 m), but not at the shallow summit. It is known that those species are sensitive to light and experiments have documented lethal effects of light, e.g. on *P. periphylla* (Jarms et al., 2002), which are in agreement with observed distribution pattern in this study. We found that the biomass of *Beroe* spp. and the four grouped hydromedusae were relatively low at the seamount summit compared to relatively high values at the flanks (main peak between 200 and 400 m) and Oceanic Reference North stations. Whether this is driven by a general avoidance of the shallow summit region or predator-prey interactions around the seamount needs further study. Further, we found relatively high pyrosome abundances at the seamount summit, but highest pyrosome densities were observed at the Oceanic Reference South and southeastern Seamount Flank stations with 0.4–0.75 ind. m^{-3} . Those abundances compare well with maximum pyrosome abundance of 0.8 ind. m^{-3} reported from a highly productive eddy core in Cape Verdean waters (Stenvers et al., 2021).

Some GZ groups are known to conduct extended diel vertical migration (DVM), changing their depth distribution on a daily basis (as reviewed in Graham et al., 2001). In our study, we found only a very weak effect of daytime on hydromedusae abundances. Similar to our results, Denda and Christiansen (2014) did not find clear day-night differences of macrozooplankton in the same area, while Hoving et al. (2020) found significant DVM only for siphonophores and *Atolla* spp. We did not investigate siphonophores, due to the problem of quantitatively collecting them with nets, while *A. wyvillei* densities were too low to allow for statistical analyses. Overall, for pooled GZ counts, no DVM patterns were detected, but clustering of different species might have masked patterns of individual species.

4.4. Gelatinous zooplankton biomass distribution

Gelatinous zooplankton (GZ) span a large size and weight range (e.g. McConville et al., 2017). In order to account for these differences, estimates of biomass are essential to allow for evaluating their ecological role and for comparisons across ecosystems (e.g. see Bar-On et al., 2018). For example, it has been shown that jellyfish and salps make up $40 \pm 34\%$ of the combined mesozooplankton and fish biomass in surface waters of the Arabian Sea during night time (Gjøsaeter, 1984). This indicates that the GZ biomass contribution can be large. In order to assess biomass, size as well as weights of organisms need to be assessed. However, due to the fragile nature of most GZ groups and their problematic preservation (e.g. as outlined in van Walraven et al., 2013),

reliable count and size data are often based on analyses of live material right after catch (e.g. see Haraldsson et al., 2013), while weight assessments and length-weight regressions are often conducted in the laboratory from preserved material. As animals are known to shrink due to preservation (e.g. Mutlu, 1996; Wetzel et al., 2005), shrinkage effects need to be considered, but often differ between species and taxa (e.g. Wetzel et al., 2005). In this study, we compared the slope of length-weight regressions from live (literature) and preserved (this study) material in order to circumvent uncertainty due to species- or taxon-specific shrinkage effects, which have not been quantified. We show that the species- or group-specific slopes of our investigated taxa do not differ significantly. Therefore, live size measurements were used to assess wet weights, which were then converted to carbon using published conversion factors (following Kiørboe, 2013; McConville et al., 2017). Note that wet weights are relatively more independent of salinity compared to dry weight for GZ (Hirst and Lucas, 1998; Kiørboe 2013). Following this approach, we show that the GZ biomass is not negligible, especially in the OMZ of Oceanic Reference South stations (400–600 m) with $28.23 \text{ mg C m}^{-2}$ (0.14 mg C m^{-3}). Also, the depth layer of 600–1000 m at the south-eastern Seamount Flank station showed a high average integrated total GZ biomass of 39 mg C m^{-2} , equivalent to 0.1 mg C m^{-3} . An investigation in the same area assessing the macrozooplankton (0.4–20 mm) with Multinets found a median biomass of $0.7\text{--}1 \text{ mg C m}^{-3}$ in the upper 100 m, with a peak biomass at the OMZ with 1.5 mg C m^{-3} (Kiko et al., 2020). Hence, our peak average biomass, representing only GZ (without siphonophores), amounted to about 10% of the total macrozooplankton biomass reported by Kiko et al. (2020), whereas our lowest average GZ biomass at the north-west seamount flank station was only 0.02 mg C m^{-3} or ca. 2% of the total macrozooplankton biomass given by Kiko et al. (2020). In comparison, the global geometric mean biomass of GZ has been estimated as 0.53 mg C m^{-3} , with averages of 0.17 and 1.6 mg C m^{-3} for the southern and northern Atlantic, respectively (Lucas et al., 2014).

In conclusion, irrespective of relatively low abundances, GZ are widespread in the Eastern Tropical North Atlantic around the Cape Verdean archipelago and may represent a substantial biomass contribution to the plankton community. While higher abundances of gelatinous zooplankton organisms investigated in this study strongly correlate with warmer waters, low oxygen concentrations do not appear to constrain their distribution.

Funding

CJ was supported by the European Union's Seventh Framework Programme for research, technological development and demonstration – Marie Curie and the Danish Council for Independent Research – Marie Curie (mobilex DFF-1325-00102B) and a research grant (00025512) from VILLUM FONDEN. The DFG provided ship time and financial support (SEAMOX).

CRediT authorship contribution statement

Florian Lüskow: Conceptualization, Methodology, Investigation, Visualization, Writing. **Bernd Christiansen:** Conceptualization, Methodology, Investigation, Writing. **Xupeng Chi:** Investigation, Commenting. **Péricles Silva:** Investigation, Commenting. **Philipp Neitzel:** Investigation, Visualization, Commenting. **Mollie E. Brooks:** Formal analysis, Visualization, Writing. **Cornelia Jaspers:** Conceptualization, Formal analysis, Visualization, Writing.

Declaration of competing interest

The authors declare that they have no known competing financial interests or personal relationships that could have appeared to influence the work reported in this paper.

Acknowledgments

Thanks are due to the captain and crew of *R/V Maria S. Merian* for the excellent collaboration. We would like to thank Ole S. Tendal, Aino L. J. Hosaia, Steven H. D. Haddock, and Gerhard Jarms for image verification of GZ specimens and Anneke Denda, Cornelia and Fritz Buchholz, Silke Janßen, Alessandra Kronschnabel, Bettina Martin, and Timo Zeimet, who conducted the MOCNESS sampling, secured the material and enabled us to work in their laboratories at the Universität Hamburg. Thanks to Manfred Kaufmann, Barbara Springer, and Neusa Pinheiro for conducting the CTD casts and help with the Winkler titration. We would like to especially thank Fabien Lombard for discussions of length-weight relationships of gelatinous zooplankton, Henk-Jan Hoving for initiation of this investigation and support, and two anonymous reviewers for constructive comments made on an earlier version of the manuscript.

Appendix A. Supplementary data

Supplementary data to this article can be found online at <https://doi.org/10.1016/j.marenvres.2022.105566>.

References

- Aristegui, J., Barton, E.D., Álvarez-Salgado, X.A., Santos, A.M.P., Figueiras, F.G., Kifani, S., Hernández-León, S., Mason, E., Machú, E., Demarcq, H., 2009. Sub-regional ecosystem variability in the Canary Current upwelling. *Prog. Oceanogr.* 83, 33–48. <https://doi.org/10.1016/j.pocean.2009.07.031>.
- Ayala, D.J., Munk, P., Lundgreen, R.B.C., Traving, S.J., Jaspers, C., Jørgensen, T.S., Hansen, L.H., Riemann, L., 2018. Gelatinous plankton is important in the diet of European eel (*Anguilla anguilla*) larvae in the Sargasso Sea. *Sci. Rep.* 8, 6156. <https://doi.org/10.1038/s41598-018-24388-x>.
- Bar-On, Y.M., Phillips, R., Milo, R., 2018. The biomass distribution on Earth. *Proc. Natl. Acad. Sci. U.S.A.* 115 (25), 6506–6511.
- Barón, K., 2019. MuMIn: Multi-Model Inference. R package. version 1.43.6. <https://CRAN.R-project.org/package=MuMIn>.
- Bolker, B.M., 2015. Linear and generalized linear mixed models. In: Fox, G.A., Negrete-Yankelevich, S., Sosa, V.J. (Eds.), *Ecological Statistics*. Oxford University Press, Oxford, UK.
- Brandt, P., Bange, H.W., Banyte, D., Dengler, M., Didwischus, S.-H., Fischer, T., et al., 2015. On the role of circulation and mixing in the ventilation of oxygen minimum zones with a focus on the eastern tropical North Atlantic. *Biogeosciences* 12, 489–512. <https://doi.org/10.5194/bg-12-489-2015>.
- Breitburg, D.L., Adamack, A., Rose, K.A., Kolesar, S.E., Decker, M.B., Purcell, J.E., et al., 2003. The pattern and influence of low dissolved oxygen in the Patuxent River, a seasonally hypoxic estuary. *Estuaries* 26 (2A), 280–297. <https://doi.org/10.1007/BF02695967>.
- Brooks, M.E., Kristensen, K., van Benthem, K.J., Magnusson, A., Berg, C.W., Nielsen, A., Skaug, H.J., Mächler, M., Bolker, B.M., 2017. glmmTMB balances speed and flexibility among packages for zero-inflated generalized linear mixed modeling. *The R J* 9 (2), 378–400.
- Buecher, E., Sparks, C., Brierley, A., Boyer, H., Gibbons, M., 2001. Biometry and size distribution of *Chrysaora hysoxcella* (Cnidaria, Scyphozoa) and *Aequorea aequorea* (Cnidaria, Hydrozoa) off Namibia with some notes on their parasite *Hyperia medusarum*. *J. Plankton Res.* 23 (10), 1073–1080.
- Burnham, K.P., Anderson, D.R., Huyvaert, K.P., 2011. AIC model selection and multimodel inference in behavioral ecology: some background, observations, and comparisons. *Behav. Ecol. Sociobiol.* 65, 23–35. <https://doi.org/10.1007/s00265-010-1029-6>.
- Décima, M., Stukel, M.R., López-López, L., Landry, M.R., 2019. The unique ecological role of pyrosomes in the Eastern Tropical Pacific. *Limnol. Oceanogr.* 64 (2), 728–743. <https://doi.org/10.1002/lno.11071>.
- Denda, A., Christiansen, B., 2014. Zooplankton distribution patterns at two seamounts in the subtropical and subtropical NE Atlantic. *Mar. Ecol. Prog. Ser.* 35 (2), 159–179. <https://doi.org/10.1111/maec.12065>.
- Diaz, R.J., 2001. Overview of hypoxia around the world. *J. Environ. Qual.* 30 (2), 275–281.
- Diaz, R.J., Rosenberg, R., 2008. Spreading dead zones and consequences for marine ecosystems. *Science* 321 (5891), 926–929. <https://doi.org/10.1126/science.1156401>.
- Diaz Briz, L., Sánchez, F., Mari, N., Mianzan, H., Genzano, G., 2017. Gelatinous zooplankton (ctenophores, salps and medusae): an important food resource of fishes in the temperate SW Atlantic Ocean. *Mar. Biol. Res.* 13 (6), 630–644. <https://doi.org/10.1080/17451000.2016.1274403>.
- Dormann, C.F., Calabrese, J.M., Guillera-Arroita, G., Matechou, E., Bahn, V., Bortoni, K., et al., 2018. Model averaging in ecology: a review of Bayesian, information-theoretic, and tactical approaches for predictive inference. *Ecol. Monogr.* 88, 485–504. <https://doi.org/10.1002/ecm.1309>.
- Gjøsaeter, J., 1984. Mesopelagic fish, a large potential resource in the Arabian Sea. *Deep-Sea Res. Part I Oceanogr. Res. Pap.* 31 (6–8), 1019–1035.
- Graham, W.M., Pag, F., Hamner, W.M., 2001. A physical context for gelatinous zooplankton aggregations: a review. *Hydrobiologia* 451 (1), 199–212.
- Grasshoff, K., 1999. Methods of nutrient analysis. In: Grasshoff, K., Kremling, K., Ehrhardt, M. (Eds.), *Methods of Seawater Analysis*, third ed. Wiley-VCH, Weinheim, pp. 61–72.
- Haraldsson, M., Jaspers, C., Tiselius, P., Aksnes, D.L., Andersen, T., Titelman, J., 2013. Environmental constraints of the invasive *Mnemiopsis leidyi* in Scandinavian waters. *Limnol. Oceanogr.* 58 (1), 37–48.
- Hardin, J., Hilbe, J., 2007. *Generalized Linear Models and Extensions*, 2nd edition. Stata Press, College Station, TX.
- Hartig, F., 2020. DHARMA: Residual Diagnostics for Hierarchical (Multi-Level/Mixed) Regression Models. R package version 0.2.7. <https://CRAN.R-project.org/package=DHARMA>.
- Hauss, H., Christiansen, S., Schütte, F., Kiko, R., Lima, M.E., Rodrigues, E., Karstensen, J., Löscher, C.R., Körtzinger, A., Fiedler, B., 2016. Dead zone or oasis in the open ocean? Zooplankton distribution and migration in low-oxygen medowater eddies. *Biogeosciences* 13, 1977–1989. <https://doi.org/10.5194/bg-13-1977-2016>.
- Henschke, N., Pakhomov, E.A., Kwong, L.E., Everett, J.D., Laiolo, L., Coghlan, A.R., et al., 2019. Large vertical migrations of *Pyrosoma atlanticum* play an important role in active carbon transport. *J. Geophys. Res. Biogeosci.* 124 (5), 1056–1070.
- Hirsch, S., Martin, B., Christiansen, B., 2009. Zooplankton metabolism and carbon demand at two seamounts in the NE Atlantic. *Deep-Sea Research II* 56 (25), 2656–2670.
- Hirst, A.G., Lucas, C.H., 1998. Salinity influences body weight quantification in the scyphomedusa *Aurelia aurita*: important implications for body weight determination in gelatinous zooplankton. *Mar. Ecol. Prog. Ser.* 165, 259–269.
- Hopcroft, R.R., Roff, J.C., 1995. Zooplankton growth rates - extraordinary production by the larvacean *Oikopleura dioica* in tropical waters. *J. Plankton Res.* 17 (2), 205–220.
- Hosaia, A., Falkenheug, T., Baxter, E.J., Pagès, F., 2017. Abundance, distribution and diversity of gelatinous predators along the northern Mid-Atlantic Ridge: a comparison of different sampling methodologies. *PLoS One* 12 (11), e0187491.
- Hoving, H.J.T., Neitzel, P., Hauss, H., Christiansen, S., Kiko, R., Robison, B.H., Silva, P., Körtzinger, A., 2020. *In situ* observations show vertical community structure of pelagic fauna in the eastern tropical North Atlantic off Cape Verde. *Sci. Rep.* 10, 21798.
- Jarms, G., Tiemann, H., Båmstedt, U., 2002. Development and biology of *Periphylla periphylla* (Scyphozoa: Coronatae) in a Norwegian fjord. *Mar. Biol.* 141 (4), 647–657.
- Karstensen, J., Stramma, L., Visbeck, M., 2008. Oxygen minimum zones in the eastern tropical Atlantic and Pacific oceans. *Prog. Oceanogr.* 77 (4), 331–350. <https://doi.org/10.1016/j.pocean.2007.05.009>.
- Kiko, R., Brandt, P., Christiansen, S., Faustmann, J., Krist, I., Rodrigues, E., et al., 2020. Zooplankton-mediated fluxes in the eastern tropical North Atlantic. *Front. Mar. Sci.* 7, 358.
- Kjørboe, T., 2013. Zooplankton body composition. *Limnol. Oceanogr.* 58 (5), 1843–1850. <https://doi.org/10.4319/lo.2013.58.5.1843>.
- Kolesar, S.E., Breitbart, D.L., Purcell, J.E., Decker, M.B., 2010. Effects of hypoxia on *Mnemiopsis leidyi*, ichthyoplankton and copepods: clearance rates and vertical habitat overlap. *Mar. Ecol. Prog. Ser.* 411, 173–188. <https://doi.org/10.3354/meps08656>.
- Kremer, P., Nixon, 1976. Distribution and abundance of ctenophore *Mnemiopsis leidyi* in Narragansett Bay. *Estuar. Coast Mar. Sci.* 4 (6), 627–639.
- Lavelle, J.W., Mohn, C., 2010. Motion, commotion, and biophysical connections at deep ocean seamounts. *Oceanography* 23 (1), 90–103.
- Lebrato, M., Jones, D.O.B., 2009. Mass deposition event of *Pyrosoma atlanticum* carcasses off Ivory Coast (west Africa). *Limnol. Oceanogr.* 54 (4), 1197–1209. <https://doi.org/10.4319/lo.2009.54.4.1197>.
- Leitner, A.B., Neumeier, A.B., Drazen, J.C., 2021. Evidence for long-term seamount-induced chlorophyll enhancements. *Sci. Rep.* 10, 12729.
- Lilley, M.K.S., Ferraris, M., Elineau, A., Berline, L., Cuvilliers, P., Gilletta, L., et al., 2014. Culture and growth of the jellyfish *Pelagia noctiluca* in the laboratory. *Mar. Ecol. Prog. Ser.* 510, 265–273.
- Lučić, D., Hure, M., Bobanović-Čolić, S., Njire, J., Vidjak, O., Onofri, I., Gangai Zovko, B., Batistić, M., 2019. The effect of temperature change and oxygen reduction on zooplankton composition and vertical distribution in a semi-enclosed marine system. *Mar. Biol. Res.* 15 (4–6), 325–342. <https://doi.org/10.1080/17451000.2019.1655161>.
- Lucas, C.H., Jones, D.O.B., Hollyhead, C.J., Condon, R.H., Duarte, C.M., Graham, W.M., et al., 2014. Gelatinous zooplankton biomass in the global oceans: geographic variation and environmental drivers. *Global Ecol. Biogeogr.* 23 (7), 701–714.
- Lüdecke, D., 2021. sjPlot: Data Visualization for Statistics in Social Science. R package version 2.8.7. <https://CRAN.R-project.org/package=sjPlot>.
- McConville, K., Atkinson, A., Fileman, E.S., Spicer, J.I., Hirst, A.G., 2017. Disentangling the counteracting effects of water content and carbon mass on zooplankton growth. *J. Plankton Res.* 39 (2), 246–256.
- McEwen, G.F., Johnson, M.W., Folsom, T.R., 1954. A statistical analysis of the performance of the Folsom plankton splitter, based on upon test observations. *Arch. Met. Geoph. Biokl. A* 7 (1), 502–527.
- Mills, C.E., Haddock, S.H.D., 2007. Ctenophora. 189–199, with 5 plates. In: Carlton, J.T. (Ed.), *Light and Smith's Manual: Intertidal Invertebrates of the Central California Coast*, fourth ed. University of California Press, Berkeley.
- Morato, T., Varkey, D.A., Damaso, C., Machete, M., Santos, M., Prieto, R., Santos, R.S., Pitcher, T.J., 2008. Evidence of a seamount effect on aggregating visitor. *Mar. Ecol. Prog. Ser.* 357, 23–32. <https://doi.org/10.3354/meps07269>.
- Mutlu, E., 1996. Effect of formaldehyde on the gelatinous zooplankton (*Pleurobrachia pileus*, *Aurelia aurita*) during preservation. *Tr. J. Zool.* 20, 423–426.

- Purcell, J.E., Breitbart, D.L., Decker, M.B., Graham, W.M., Youngbluth, M.J., Raskoff, K. A., 2001. Pelagic Cnidarians and Ctenophores in Low Dissolved Oxygen Environments: a Review. Coastal Hypoxia: Consequences for Living Resources and Ecosystems. Coastal and Estuarine Studies. American Geophysical Union, pp. 77–100.
- R Core Team, 2020. A Language and Environment for Statistical Computing. R Foundation for Statistical Computing, Vienna, Austria. <http://www.R-project.org/>.
- Remsen, A., Hopkins, T.L., Samson, S., 2004. What you see is not what you catch: a comparison of concurrently collected net, Optical Plankton Counter, and Shadowed Image Particle Profiling Evaluation Recorder data from the northeast Gulf of Mexico. *Deep-Sea Res. Part I Oceanogr. Res. Pap.* 51 (1), 129–151.
- Richardson, A.J., Bakun, A., Hays, G.C., Gibbons, M.J., 2009. The jellyfish joyride: causes, consequences and management responses to a more gelatinous future. *Trends Ecol. Evol.* 24 (6), 312–322. <https://doi.org/10.1016/j.tree.2009.01.010>.
- Robison, B.H., 2004. Deep pelagic biology. *J. Exp. Mar. Biol. Ecol.* 300 (1–2), 253–272. <https://doi.org/10.1016/j.jembe.2004.01.012>.
- Schielzeth, H., 2010. Simple means to improve the interpretability of regression coefficients. *Methods Ecol. Evol.* 1, 103–113. <https://doi.org/10.1111/j.2041-210X.2010.00012.x>.
- Sieburth, J.M., Smetacek, V., Lenz, J., 1978. Pelagic ecosystem structure: heterotrophic compartments of the plankton and their relationship to plankton size fractions. *Limnol. Oceanogr.* 23 (6), 1256–1263. <https://doi.org/10.4319/lo.1978.23.6.1256>.
- Skjoldal, H.R., Wiebe, P.H., Postel, L., Knutsen, T., Kaartvedt, S., Sameoto, D.D., 2013. Intercomparison of zooplankton (net) sampling systems: results from the ICES/GLOBEC sea-going workshop. *Prog. Oceanogr.* 108, 1–42.
- Slater, W.L., Pierson, J.J., Decker, M.B., Houde, E.D., Lozano, C., Seuberling, J., 2020. Fewer Copepods, Fewer Anchovies, and More Jellyfish: How Does Hypoxia Impact the Chesapeake Bay Zooplankton Community? *Diversity* 12 (1), 35.
- Stenvers, V.I., Hauss, H., Osborn, K.J., Neitzel, P., Merten, V., Scheer, S., et al., 2021. Distribution, associations and role in the biological carbon pump of *Pyrosoma atlanticum* (Tunicata, Thaliacea) off Cabo Verde, NE Atlantic. *Sci. Rep.* 11 (1), 9231.
- Stramma, L., Johnson, G.C., Sprintall, J., Mohrholz, V., 2008. Expanding oxygen-minimum zones in the tropical oceans. *Science* 320, 655–658. <https://doi.org/10.1126/science.1153847>.
- Svetlichny, L.S., Abolmasova, G.I., Hubareva, E.S., Finenko, G.A., Bat, L., Kideys, A.E., 2004. Respiration rates of *Beroe ovata* in the black sea. *Mar. Biol.* 145 (3), 585–593.
- Thuesen, E.V., Rutherford Jr., L.D., Brommer, P.L., Garrison, K., Gutowska, M.A., Towanda, T., 2005. Integral oxygen promotes hypoxia tolerance of scyphomedusae. *J. Exp. Biol.* 208, 2475–2482. <https://doi.org/10.1242/jeb.01655>.
- Tranter, D.J., 1962. Zooplankton abundance in Australasian waters. *Aust. J. Mar. Freshw. Res.* 13, 106–142.
- van Walraven, L., Langenberg, V.T., van der Veer, H.W., 2013. Seasonal occurrence of the invasive ctenophore *Mnemiopsis leidyi* in the western Dutch Wadden Sea. *J. Sea Res.* 82, 86–92.
- Wetzel, M.A., Leuchs, H., Koop, J.H.E., 2005. Preservation effects on wet weight, dry weight, and ash-free dry weight biomass estimates of four common estuarine macro-invertebrates: no difference between ethanol and formalin. *Helgol. Mar. Res.* 59, 206–213.
- Whittingham, M.J., Stephens, P.A., Bradbury, R.B., Freckleton, R.P., 2006. Why do we still use stepwise modelling in ecology and behaviour? *J. Anim. Ecol.* 75, 1182–1189. <https://doi.org/10.1111/j.1365-2656.2006.01141.x>.